

Synthesis and Characterization of Graft Copolymers with Molecularly Uniform Urethane-Based Side Chains with Special Structural Elements

Claus D. Eisenbach* and Torsten Heinemann

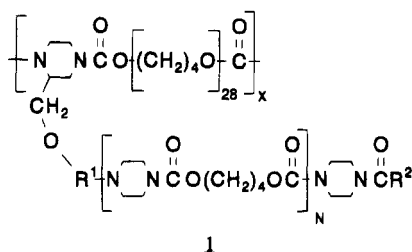
Makromolekulare Chemie II, Universität Bayreuth, D-95440 Bayreuth, Germany

Received December 29, 1994; Revised Manuscript Received March 13, 1995*

ABSTRACT: Graft copolymers consisting of poly(oxytetramethylene) primary chain and distinctly engineered molecularly uniform oligo(*N*-alkylurethane) side chains with two constitutional units were synthesized and investigated by thermal and dynamic mechanical analysis. Microphase-separated systems with semicrystalline oligourethane hard domains and exhibiting the characteristic properties of thermoplastic elastomers were observed for graft copolymers either with a spacer between the polyether backbone and the side chain or with specifically interacting graft end groups. The properties were correlated with contributions of special side chain interactions and main chain-side chain coupling to the segregation and packing of the oligourethane branches.

Introduction

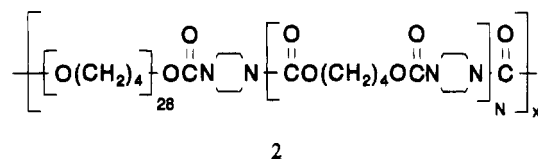
Graft copolymers **1a** with polyether main chain and molecularly uniform oligourethane side chains were accessible by a polycondensation reaction of molecularly uniform α,α' -bifunctional oligourethane macromonomers and telechelic poly(oxytetramethylene).¹



1	R ¹	R ²	N
a		-OCH ₃	2,3,4,7
b		-OCH ₃	2
c		-OCH ₃	2
d			2
e			2

For $N > 2$ they were thermoplastic elastomers; i.e., a microphase separation had occurred where the grafts formed semicrystalline hard domains dispersed in a continuous soft phase formed by the polyether backbone polymer.^{1,2} Interactions between the oligourethane grafts of **1a**, not capable of forming any hydrogen bond, allowed the formation of an ordered superstructure when the side chains had exceeded a critical length.¹ A

comparison with segmented poly(ether-urethane) elastomers **2** (cf. refs 3-6) with molecularly uniform hard



segments built analogously to the graft, i.e., based on monomers piperazine, 1,4-butanediol, and phosgene (1,4-piperazinediylcarbonyloxytetramethylene-oxycarbonyl repeating units) showed that the crystallization behavior of the grafts was strongly limited due to steric interactions of the covalently linked main chain.¹

From these findings the question arose if and how it would be possible to influence the formation of the ordered superstructure by making use of specific features of the architecture of the graft copolymer **1**. A reasonable approach was to introduce a spacer R^1 between the polyether main chain and the polyurethane grafts and/or specifically interacting end groups R^2 of the grafts. One could expect that with specific end groups, e.g. capable of forming hydrogen bridge bonds (**1d**), or by varying the distance of the crystallizable grafts to the main chain (**1b,c**), the crystallization behavior of the grafts and with that the material properties of the polymers could be influenced. In this paper we report on how the microphase separation and thus the material properties of graft copolymers were effectively altered by such slight changes in the constitution of the side chain.

Results and Discussion

The combination of a stepwise synthesis for α,α' -bifunctional oligourethane building blocks by using protective groups with a subsequent substitution polycondensation gave access to exactly defined graft copolymers **1** with molecularly uniform urethane-based side chains with special structural units, placed at any part in the graft.

The synthesis of graft copolymers **1b,c** with different distances between the ether main chain and the molecularly uniform oligourethane side chain followed the

* Abstract published in *Advance ACS Abstracts*, May 1, 1995.

strategy outlined in Scheme 1. Dibenzyl 2-[(chloroformyl)oxy)methylene]-*N,N'*-piperazinedicarboxylate (**5**),¹ i.e., 2-(hydroxymethyl)piperazine^{7,8} with blocked amino groups and an activated (by reaction with phosgene) hydroxy group was reacted with amino alcohols **7a/b** of different lengths; due to the different reactivities of the amino and hydroxy group toward the chloroformate, **8a/b** was the preferred reaction product and almost no carbonate was formed. **8a/b** was reacted with phosgene and then with **10** to give **11a/b**. The molecularly uniform amino-terminated oligourethane **10** was obtained from the starting materials piperazine, 1,4-butanediol, and phosgene by a stepwise synthesis using protective groups by applying a synthetic strategy already described.^{4,9} Removal of the protective groups in **11a/b** by catalytic hydrogenation gave the macromonomers **12a/b**, which were reacted with α -(chloroformyl)- ω -(chloroformyl)poly(oxytetramethylene), **13** (bis(chloroformate) of POTM, $M_n = 2000$) (cf. ref 1) to give the graft copolymers **1b,c** of different distances between the main chain and grafts.

Graft copolymers **1d,e** with molecularly uniform side chains but different end groups were obtained as described in Scheme 2. At a pH of 3, one amino group of piperazine could be reacted with benzyl chloroformate to give **14**,^{4,9} which was reacted with 4-(methoxycarbonyl)phenyl chloroformate to give the intermediate **15**, from which **16** was obtained by catalytic hydrogenation. Alternatively, **14** could be reacted with phosgene, the resulting carbamoyl chloride¹⁰ giving **19** after conversion with gaseous methylamine to the urea **18** and catalytic hydrogenation. **16** or **19** was reacted with the chloroformate **20**.^{4,9} After removal of the benzyloxycarbonyl group of **21a/b** (catalytic hydrogenation), reaction with **5**, and removal of the protective groups, the obtained macromonomers **24a/b** were reacted with **13** to yield the graft copolymers **1d,e** with molecularly uniform side chains and different end groups as compared to **1a** ($N = 2$).

The effect of varying the distance between the molecularly uniform (and in principle crystallizable) grafts and polyether main chain by means of an α,ω -amino alcohol based spacer is illustrated in the DSC traces depicted in Figure 1. The graft copolymer **1a** ($N = 2$, curve 2), with grafts (methylurethane end group) directly linked to the backbone chain did not form a multiphase system; i.e., the oligourethane side chains have not segregated to semicrystalline hard domains dispersed in a continuous soft phase of the polyether backbone. This could be derived from the fact that only one relatively strong melting endotherm was observed at the same temperature where the unsubstituted polyether, i.e., semicrystalline poly(oxytetramethylene) (POTM, $M_n = 55\,000$, curve 1) melted.¹ In contrast to this, the graft copolymers **1b,c** with the same number of 1,4-piperazinediylcarbonyloxytetramethyleneoxy-carbonyl repeating units but with spacers (**1b**, curve 3; **1c**, curve 4) between the oligourethane side chain and the polyether backbone were characterized by endotherms at higher temperatures ($T_m = 338$ and 372 K, respectively) which have to be assigned to the melting of semicrystalline hard domains. In this context it has to be considered that the hard domains could not solely comprise urethane side chains but partly urethane functions belonging to the backbone branching site, too; this would be favored by their immobilization in the interphase as a consequence of urethane side chain crystallization (see Figure 2b). **1c** melted in the same temperature range as the segmented multiblock copolymer **2** ($N = 2$; curve 7 in Figure 1: two endotherms at

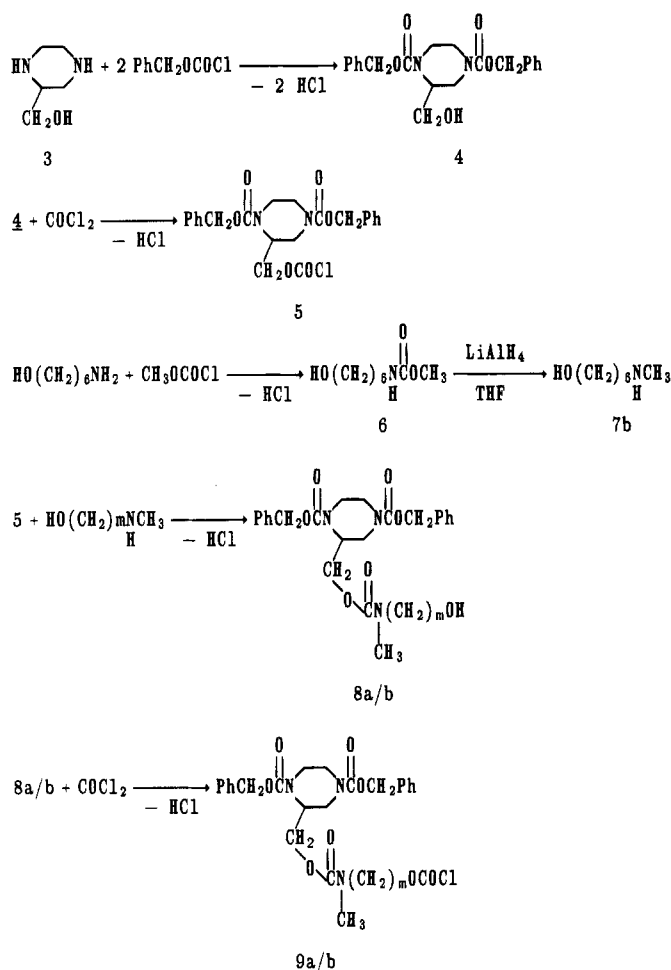
$T_m = 352$ and 371 K)⁴ with the same number of repeating units per hard segment as in the side chains of **1c**. This illustrated that the restrictions to form a microphase-separated system in graft copolymers of short, crystallizable side chains could be overcome by introducing a sufficiently long spacer which allowed the formation of hard domain crystallites similar to those in a corresponding segmented block copolymer. Reducing the spacer lengths as in **1b** (compared to **1c**) limited the microphase separation and thus resulted in lowering the hard domain melting temperature.

The melting enthalpies ΔH_m of the hard domain melting were drastically lower in the graft copolymers **1b,c** (**1b**; 1.6 J/g; **1c**, 2.5 J/g) than for the linear poly(ether urethane) **2** ($N = 2$; 12.8 J/g). For these differences probably a disturbance of the packing of the side chains by sterical interaction with the covalently linked polymer backbone was responsible. The idealized packing model of the oligourethane grafts which is similar to the hard segment packing in linear polyurethane elastomers (Figure 2a) (cf. refs 4, 6, and 11) is represented in Figure 2b. Without a spacer, the repeating units next to the backbone could not participate in the formation of hard domain crystallites because of the sterical and conformational restrictions as well as the confined space for the methylurethane end group at the branching, as has been discussed elsewhere.¹ The possible packing of such short oligourethane grafts as shown in Figure 2c would not lead to sufficiently stable hard domains. Thus the graft copolymer **1a** with only two repeating units in the graft and no spacer was obviously not capable of forming a well-microphase-separated system, and from the glass transition temperature $T_g = 197$ K of the polyether soft phase a fraction of about 50% of oligourethane grafts dispersed in the soft phase was calculated by means of the Gordon–Taylor equation (cf. ref 1); the decrease in the soft phase T_g upon introducing a spacer (**1b**, $T_g = 195$ K; **1c**, $T_g = 192$ K) also indicated the spacer effect on the microphase separation and hard domain formation, which corresponded to about 90% of the oligourethane side chains segregated to hard domains in the case of **1c**.

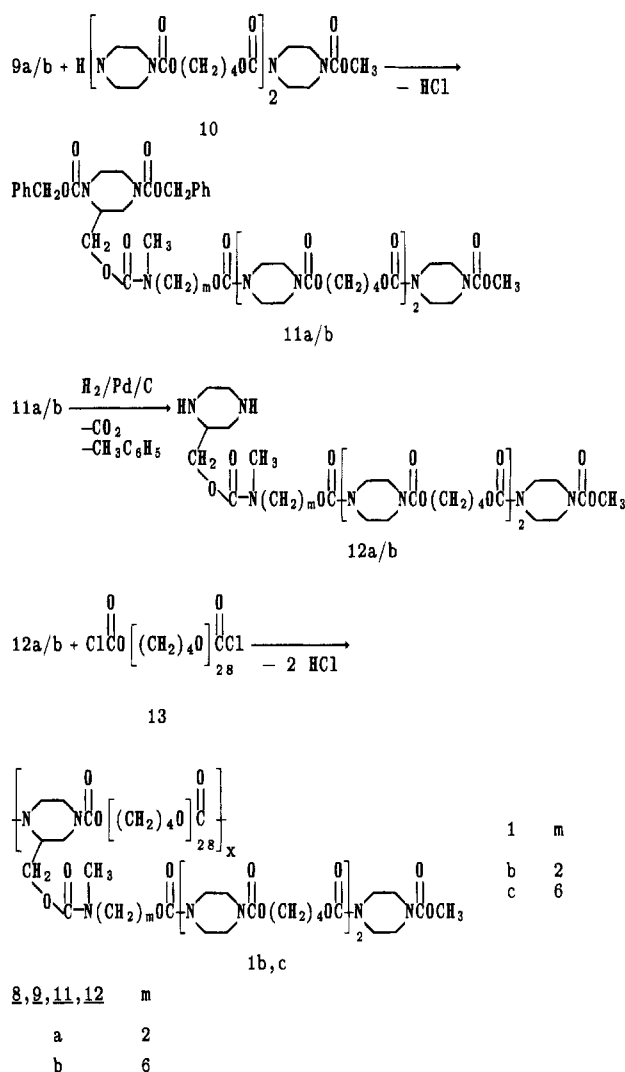
The suppression of POTM backbone crystallization as going along with microphase separation, i.e., the formation of hard domains, was in accordance with the presence of an amorphous soft phase in microphase-separated segmented polyurethanes (such as sketched in Figure 2a) as long as the molecular weight M_n of (in principle crystallizable) soft segments between hard segments did not exceed a critical value of $M_n \sim 3000$;^{11,12} the molecular weight of the starting POTM was $M_n = 2000$, and the graft copolymer synthesis via condensation polymerization excluded any prechain extension.¹ Besides, when the poly(*N*-alkylurethane) grafts have formed crystalline domains, the Y-shaped conformation of the backbone at the branching site on the top and bottom surface of the semicrystalline hard domains (see Figure 2b,c) should oppose polyether backbone crystallization, just as the crystallization was suppressed in 2,4-toluenediyl diisocyanate (2,4-TDI) extended POTM because of the disymmetrical substitution pattern of 2,4-TDI.¹³

The interpretation of the endotherms in curves 3 and 4 in Figure 1 as a melting of semicrystalline hard domains was confirmed by the analysis of the dynamic mechanical properties of the polymers discussed so far (Figure 3). Whereas the temperature dependence of the storage modulus G' of the graft copolymer **1a** ($N = 2$) without spacer was characterized by a constant decrease

Scheme 1



after passing the glass transition of the polymer backbone at about $T_g = 200$ K and then a flowing after the melting of polyether crystallites ($T_m = 300$ K), the curves of **1b,c** showed a small but characteristic plateau region of thermoplastic elastomers at temperatures higher than 300 K until the hard domains melted. Both graft copolymers are thermoplastic elastomers, as are the segmented multiblock copolymers **2**,³⁻⁵ of which ($N = 2$) the dynamic mechanical behavior is also depicted in Figure 3. The softening temperature associated with hard domain melting (the discrepancies between the melting temperatures as observed in the DSC experiments are due to the differences in the measuring method) increased with increasing spacer length. Simultaneously, the modulus in the elastomer regime increased which is in agreement with the improved microphase separation in the graft copolymer **1c** as compared to **1b**, resulting in a higher hard domain filler volume fraction for **1c**. The still somewhat higher modulus of the corresponding polyether urethane **2** ($N = 2$) in the plateau region and the higher softening temperature (cf. ref 4) may be explained by both a higher perfection in the hard segment packing and different responses of the different hard domain topologies (see Figure 2a,c) in linear segmented block copolymers and branched graft copolymer elastomers to the thermomechanical treatment. The sharper decrease and lower level of the G' vs temperature curve in the temperature region between the polyether glass transition (T_g approximately 200 K) and polyether soft seg-

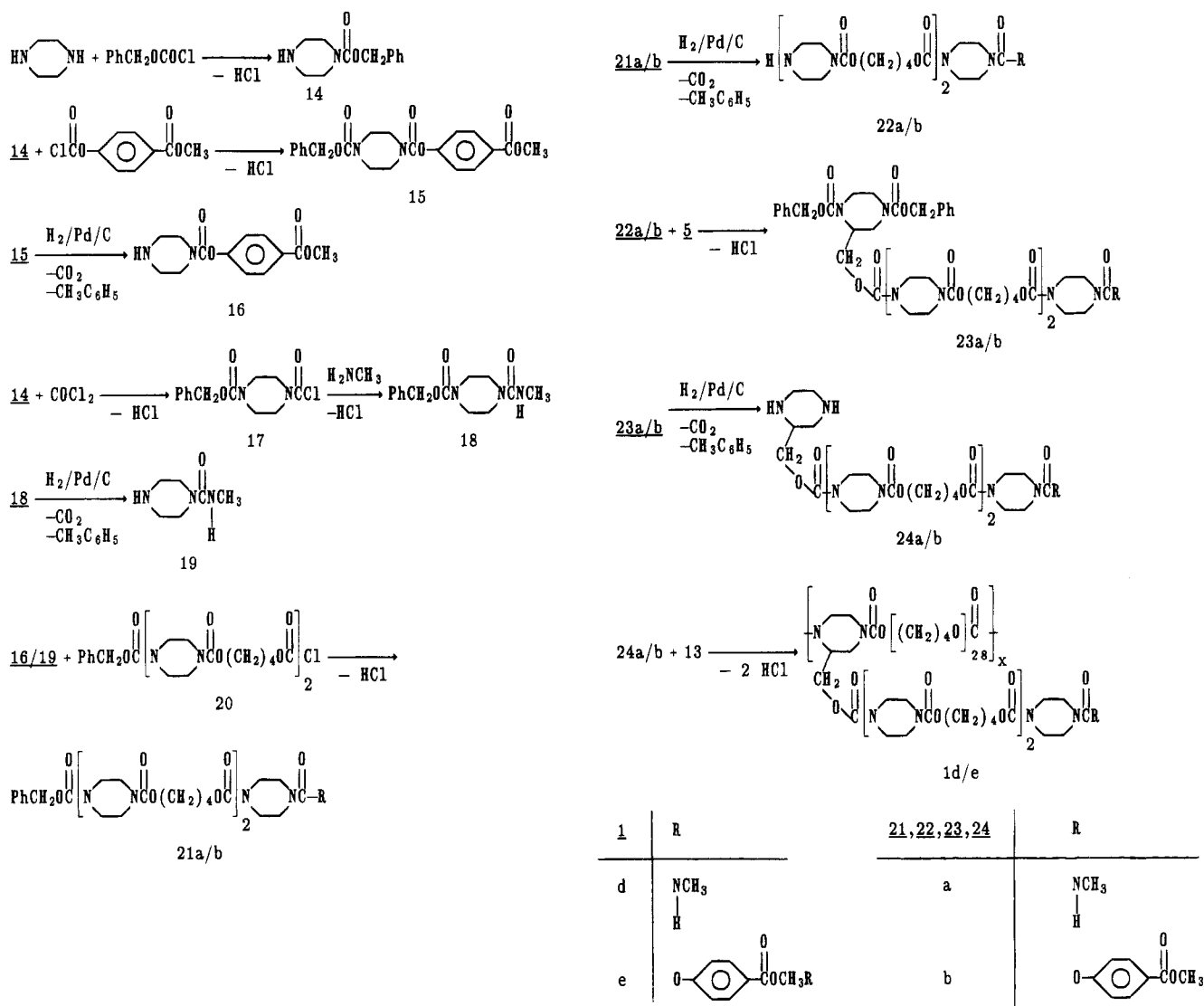


ment crystallite melting (completed at about 300 K, see also POTM curve in Figure 1 and $\tan \delta$ temperature dependencies) is also explained by the presence of more perfect hard domains (cf. ref 14).

Besides varying the distance between side chains and backbone, the formation of ordered superstructures by the graft copolymers was distinctively influenced by the end groups as revealed from the comparison of a series of graft copolymers without spacer between the polyether backbone and the same oligourethane graft ($N = 2$ repeating units) but with methylurethane (**1a**), methylurea (**1d**), or [4-((carbonyloxy)methyl)phenyl]urethane (**1e**) graft end groups. This was first evident from the melting endotherms seen in the DSC traces of **1d** ($T_m = 321$ K) and **1e** ($T_m = 324$ K), curves 5 and 6 in Figure 1, which represent the melting of hard domains formed by microphase-separated oligourethane grafts, as already discussed in detail for the graft copolymers **1b,c** (see above).

Obviously, the replacement of the methylurethane end group of **1a** ($N = 2$) by a urea end group in **1d**, which was only a minor change in the overall constitution of the graft but opened the possibility of hydrogen bond formation, was sufficient not only to stabilize the microphase-separated system but also to cause oligourethane graft crystallization. This was supported by the occurrence of the stretching vibration band of the hydrogen-bonded NH group at 3300 cm⁻¹ and also by the shoulder of the free NH groups at the high-frequency side at 3400 cm⁻¹ (Figure 4; cf. ref 15); a detailed

Scheme 2



analysis of the carbonyl band region with the emphasis on elucidating the participation of urea and/or urethane carbonyls in the hydrogen bond formation was not possible because of the overlaying band pattern. The replacement of the methyl group in the methylurethane graft end group of **1a** ($N = 2$) by an aromatic constitutional unit in **1e**, allowing π - π interactions, also led to the formation of a semicrystalline hard phase (curve 6, Figure 1). This clearly demonstrated the impact of specifically interactive groups on the function and stabilization of a microphase-separated system. Similarly as observed for **1b,c** in comparison to **1a** ($N = 2$) the polyether soft phase T_g was lowered for **1d** (195 K) as well as for **1e** (194 K). However, the modification of the graft end group was less effective on the microphase separation than the introduction of a spacer between the polyether backbone and the polyurethane graft reflected from the hard domain melting temperature of **1d,e**, which was not as high as in the case of **1b,c**. On the other hand, the melting enthalpies ΔH_m (**1d**, 10 J/g; **1e**, 9.2 J/g) were distinctively higher than in the case of **1b,c**, indicating the relatively strong interaction forces of the specific graft end groups.

The dynamic mechanical properties of the three graft copolymers (**1a** ($N = 2$), **1d**, and **1e**) with different end groups are compared in Figure 5. As already mentioned, **1a** ($N = 2$) showed no elastomeric properties, whereas the temperature dependence of the storage

modulus of both **1d** and **1e** was characterized by a distinct rubbery plateau region which extended to about 20 K above POTM melting. The sharper decrease and lower level of the G' vs temperature curve of **1e** as compared to **1d** between the polyether glass transition (T_g approximately 200 K) and hard domain melting temperature (T_m approximately 320 K) is felt to be associated with the particularities of hydrogen bond formation of the urea end group in this system. The final drop of the modulus and flowing of the thermoplastic graft copolymer elastomers **1d,e**, as caused by the melting of the hard domains, occurred at the same temperature but at a lower temperature than observed for **1b,c**, which was in agreement with the DSC data.

In conclusion, the above studies elucidated that relatively simple and small variations of the constitutional units of polyether graft copolymers with urethane-based side chains caused distinct modifications of the ordered superstructure formed by specific interactions of the grafts. The material properties could be influenced by the chain architecture which opened interesting perspectives for the design of graft copolymer architectures^{16,17} and of tailor-made polymer materials in general.

Experimental Part

Measurements. NMR spectra were obtained with a Bruker AC250 spectrometer using TMS as the internal standard.

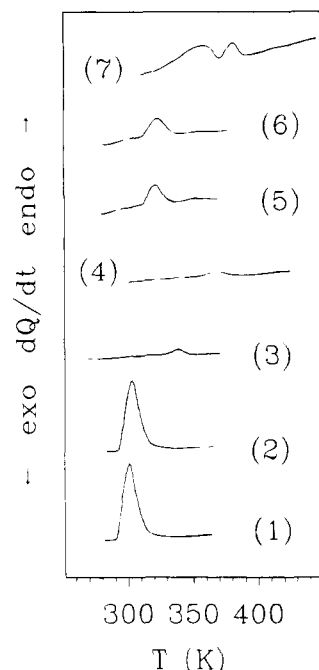


Figure 1. DSC curves of poly(oxytetramethylene) (POTM, $M_n = 55\,000$, curve 1), of graft copolymers with a polyether backbone and molecularly uniform oligourethane side chains consisting of two 1,4-piperazinediylcarbonyloxymethyl-eneoxycarbonyl repeating units without (**1a** ($N = 2$), curve 2) and with short (**1b**, curve 3) or longer spacer (**1c**, curve 4), of graft copolymers without spacer but with methylurea (**1d**, curve 5) or 4-[(carbonyloxy)methyl]phenyl (**1e**, curve 6) graft end groups, and of the segmented polyether urethane **2** ($N = 2$, curve 7 (cf. ref 4)); heating rate 20 K/min.

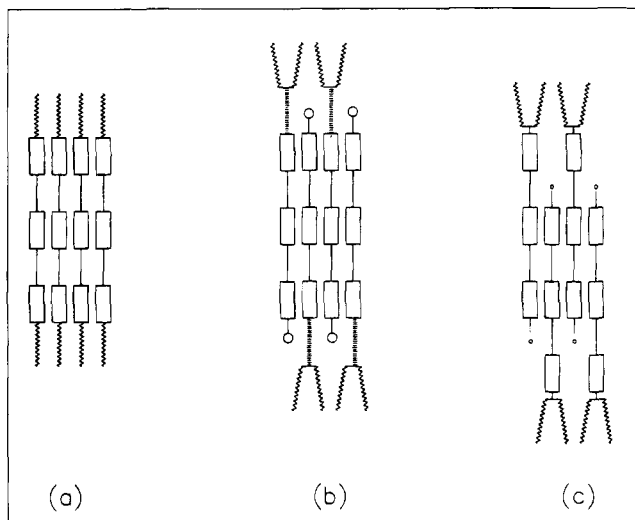


Figure 2. Schematic representation of the packing of the hard segments of the segmented polyether urethane elastomer **2** ($N = 2$, a; cf. refs 4 and 11) and the two possibilities of the packing of the oligourethane side chains of the graft copolymer **1b,c** with spacer (b) and of **1a** ($N = 2$) without spacer (c; cf. ref 1) between the polyether backbone and the oligourethane graft: \square = 1,4-piperazinediyl, $-$ = carbonyloxymethyl, \sim = POTM chain, \equiv = spacer.

IR spectra were obtained with a FT-IR spectrometer Bio-RAD Digilab Division 3240-SPC FTS-40.

Differential scanning calorimetry (DSC) was performed with a Perkin-Elmer DSC II; cyclohexane, dodecane, benzene, indium, and tin were used as calibration standards, and the sample weight was 2–5 mg.

Dynamic mechanical measurements were carried out with a Brabender torsion automat by using solution (CHCl_3) cast

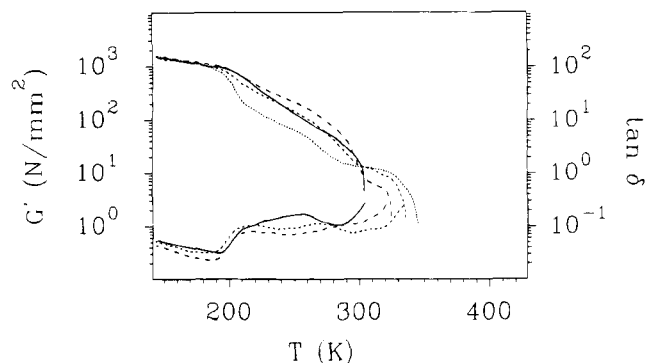


Figure 3. Dynamic mechanical properties of the graft copolymers with polyether main chain and uniform oligourethane side chains **1a** ($N = 2$, $-$), **1b** ($- -$), **1c** ($- \cdot - \cdot$), and the segmented polyurethane elastomer **2a** ($N = 2$, $\cdot \cdot \cdot$). G' = storage modulus, $\tan \delta$ = logarithmic decrement.

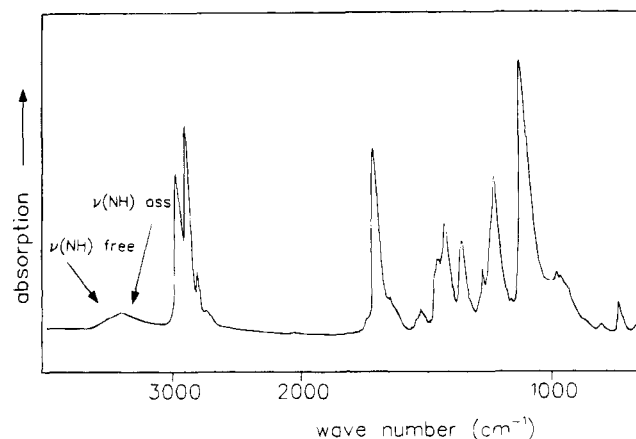


Figure 4. FT-IR spectrum of the graft copolymer **1d** (film cast from CH_2Cl_2 solution on a NaCl plate).

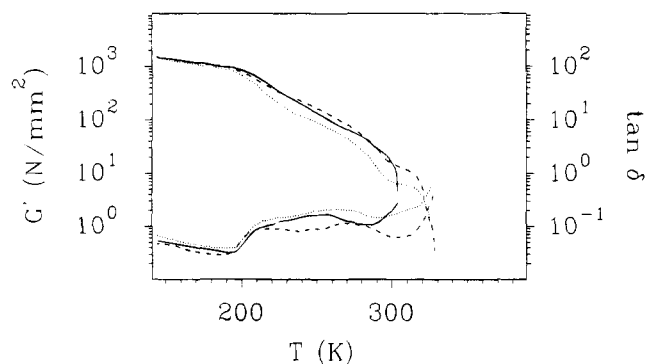


Figure 5. Dynamic mechanical properties of the graft copolymers with polyether main chain and uniform oligourethane side chains **1a** ($N = 2$, $-$), **1d** ($- -$), and **1e** ($\cdot \cdot \cdot$). G' = storage modulus, $\tan \delta$ = logarithmic decrement.

films ca. $10 \times 50 \times 1$ mm in size (temperature range 143–450 K, heating rate 1 K/min, frequency ca. 10 Hz).

[(1-Hydroxy-6-hexyl)amino]carboxymethane (6). A 25 g (0.213 mol) sample of 6-amino-1-hexanol (Aldrich) was charged into a mixture of 100 mL of CH_2Cl_2 and 220 mL of aqueous 1 M Na_2CO_3 , and 15 mL (18.4 g, 0.194 mol) of methyl chloroformate (Fluka) was dropwise added within 30 min at 0 °C under stirring. The organic phase was separated after 1 h of stirring, and the aqueous phase was extracted with 50 mL of CH_2Cl_2 ; the combined organic phases were washed twice with 50 mL of 2 M HCl, 50 mL of 10% NaHCO_3 , and then 100 mL of H_2O and dried. Evaporation of the solvent gave 20 g of crystalline **6**; yield 59%. $^1\text{H-NMR}$ (CDCl_3): δ = 1.36 (m; $\text{CH}_2\text{CH}_2\text{CH}_2\text{CH}_2$, 4H), 1.50 (m; $\text{CH}_2\text{CH}_2\text{CH}_2\text{CH}_2$, 4H), 3.16 (t; CH_2NH , 2H), 3.60 (t; HOCH_2 , 2H), 3.67 (s; COOCH_3 , 3H).

6-(Methylamino)-1-hexanol (7b) (cf. Refs 18–20). A solution of 20 g (0.114 mol) of **6** in 40 mL of THF was slowly

dropped into 6 g (0.157 mol) of LiAlH_4 (Merck) in 200 mL of THF, and the mixture was refluxed for 16 h, cooled to room temperature, and charged with 30 mL of H_2O ; the white precipitate was filtered off and washed twice with 100 mL of THF. The organic phases were evaporated, and the residue was distilled in vacuo; boiling point (0.01 mbar) 89–92 °C; yield 73%. $^1\text{H-NMR}$ (CDCl_3): δ = 1.39 (m; $\text{CH}_2\text{CH}_2\text{CH}_2\text{CH}_2$, 4H), 1.44 (m; $\text{CH}_2\text{CH}_2\text{CH}_2\text{CH}_2$, 4H), 2.35 (s; HNCH_3 , 3H), 2.50 (t; CH_2NH , 2H), 3.52 (t; CH_2OH , 2H).

Dibenzyl 2-((((Chloroformyl)oxy)alkyl)methylamino)-carbonyl)oxy)methylene]piperazine-*N,N'*-dicarboxylate (9a/b). The synthesis of 9a/b started from 5 (obtained from 3 as described earlier¹) by condensation with (methylamino)ethanol (Fluka) 7a and 7b, respectively, to obtain the intermediate products 8a,b, which were subsequently reacted with an excess of phosgene. A 4 g (9.1 mmol) or 3.2 g (7.1 mmol) sample of 5 in 20 mL of CHCl_3 was dropped into 1 g (13.3 mmol) of 7a or 1.3 g (9.9 mmol) of 7b in 50 mL of CH_2Cl_2 followed by dropwise addition of 20 mL of aqueous 1 M Na_2CO_3 . After 1 h of stirring, the organic phases were separated, the aqueous phase was washed twice with CH_2Cl_2 , and the combined organic phases were dried and evaporated; yield 75% (8a) and 76% (8b). $^1\text{H-NMR}$ (CDCl_3 , 25 °C): 8a δ = 2.82 (s; CH_3 , 3H), 2.9–3.2, 3.9–4.5 (2m; $\text{N-CH}_2\text{-CH}_2\text{-N}$, $\text{N-CH-CH}_2\text{-N}$, CHCH_2 , 9H), 4.34 (t; CH_2OCOC , 2H), 5.14 (s; PhCH_2 , 4H), 7.34 (m; PhCH_2 , 10H); 8b δ = 1.26–1.70 (m; $\text{CH}_2(\text{CH}_2)_4\text{CH}_2$, 8H), 2.82 (s; CH_3 , 3H), 2.9–3.2, 3.9–4.5 (2m; $\text{N-CH}_2\text{-CH}_2\text{-N}$, $\text{N-CH-CH}_2\text{-N}$, CHCH_2 , $\text{N}(\text{CH}_3)\text{CH}_2$, 11H), 3.64 (t; CH_2OH , 2H), 5.14 (s; PhCH_2 , 4H), 7.34 (m; PhCH_2 , 10H).

The phosgenation of 8a/b was carried out similarly as described for 5¹ and gave 9a/b in quantitative yield. $^1\text{H-NMR}$ (CDCl_3 , 25 °C): 9a δ = 2.87 (s; CH_3 , 3H), 3.09 (t; $\text{CH}_2\text{CH}_2\text{O}$, 2H), 3.2–3.5, 3.9–4.5 (2m; $\text{N-CH}_2\text{-CH}_2\text{-N}$, $\text{N-CH-CH}_2\text{-N}$, CHCH_2 , 9H), 4.34 (t; CH_2OCOC , 2H), 5.14 (s; PhCH_2 , 4H), 7.34 (m; PhCH_2 , 10H); 9b δ = 2.87 (s; CH_3 , 3H), 3.09 (t; $\text{CH}_2\text{CH}_2\text{O}$, 2H), 3.2–3.5, 3.9–4.5 (2m; $\text{N-CH}_2\text{-CH}_2\text{-N}$, $\text{N-CH-CH}_2\text{-N}$, CHCH_2 , 9H), 4.34 (t; CH_2OCOC , 2H), 5.14 (s; PhCH_2 , 4H), 7.34 (m; PhCH_2 , 10H).

The synthesis of the macromonomers 12a/b starting from 9a/b and 10⁹ and the polycondensation reaction to yield the graft copolymers 1b,c were carried out as described earlier;¹ the molar mass (number average) of the graft copolymers varied between 30 000 and 35 000 g/mol, as determined by GPC measurement (polystyrene calibration). Macromonomer yield after recrystallization from ethanol: 60% (12a) and 94% (12b). $^1\text{H-NMR}$ (CDCl_3 , 25 °C): 12a δ = 1.73 (m; $\text{OCH}_2\text{CH}_2\text{CH}_2\text{-CH}_2\text{O}$, 8H), 2.3–2.9 (m; $\text{N-CH}_2\text{CH}_2\text{-N-CH}_2\text{CH}$, 7H), 2.90 (s; NCH_3 , 3H), 3.25 (t; $\text{NCH}_2\text{CH}_2\text{O}$, 2H), 3.46 (s; $\text{N}(\text{CH}_2\text{-})(\text{CH-})$, 24H), 3.71 (s; COOCH_3 , 3H), 3.98 (2d; $>\text{CHCH}_2\text{OCON}<$, 2H), 4.14 (m; $\text{OCH}_2\text{CH}_2\text{CH}_2\text{CH}_2\text{O}$, 8H), 4.22 (m; $\text{NCH}_2\text{CH}_2\text{O}$, 2H); 12b δ = 1.36 (m; $\text{CH}_2\text{CH}_2\text{CH}_2\text{CH}_2\text{CH}_2\text{CH}_2$, 4H), 1.54 (m; NCH_2CH_2 , 2H), 1.65 (m; $\text{CH}_2\text{CH}_2\text{CH}_2\text{CH}_2\text{CH}_2\text{CH}_2\text{O}$, 2H), 1.73

(m; $\text{OCH}_2\text{CH}_2\text{CH}_2\text{CH}_2\text{O}$, 8H), 2.3–2.9 (m; $\text{N-CH}_2\text{CH}_2\text{-N-CH}_2\text{CH}$, 7H), 2.95 (s; NCH_3 , 3H), 3.25 (t; $\text{NCH}_2\text{CH}_2\text{O}$, 2H), 3.46 (s; $\text{N}(\text{CH}_2\text{-})(\text{CH-})$, 24H), 3.71 (s; COOCH_3 , 3H), 3.98 (2d; $>\text{CHCH}_2\text{OCON}<$, 2H), 4.14 (m; OCH_2CH_2 , 10H). $^{13}\text{C-NMR}$ (CDCl_3 , 25 °C): 12a δ = 25.5 ($\text{OCH}_2\text{CH}_2\text{CH}_2\text{CH}_2\text{O}$), 35.4 (NCH_3), 43.5 ($\text{N}(\text{CH}_2\text{-})(\text{CH-})$), 46.3, 46.4, 48.9, 54.9 ($\text{N-CH}_2\text{CH}_2\text{-N-CH}_2\text{CH}$), 47.7 ($\text{NCH}_2\text{CH}_2\text{O}$), 52.8 (COOCH_3), 62.9 ($\text{NCH}_2\text{CH}_2\text{O}$), 65.0 ($\text{OCH}_2(\text{CH}_2)_2\text{CH}_2\text{O}$), 67.5 ($>\text{CHCH}_2\text{OCON}<$), 155.1, 155.2, 155.6 (CO); 12b δ = 25.5 ($\text{OCH}_2\text{CH}_2\text{CH}_2\text{CH}_2\text{O}$), 26.7, 27.0, 28.7, 29.0 ($\text{CH}_2\text{CH}_2\text{CH}_2\text{CH}_2\text{CH}_2\text{CH}_2$), 34.4 (NCH_3), 36.1 ($\text{N}(\text{CH}_3)\text{CH}_2$), 43.5 ($\text{N}(\text{CH}_2\text{-})(\text{CH-})$), 46.3, 46.4, 48.9, 54.9 ($\text{N-CH}_2\text{CH}_2\text{-N-CH}_2\text{CH}$), 52.8 (COOCH_3), 65.0, 65.4 (OCH_2), 67.1 ($>\text{CHCH}_2\text{OCON}<$), 155.1, 155.2, 155.6 (CO). IR (KBr): 12a and 12b $\nu(\text{C=O})$ 1701 cm^{-1} .

Methyl 4-(((4-(Benzyloxycarbonyl)piperazin-1,4-diyl)-carbonyl)oxy)benzoate (15). A 4.6 g (0.0215 mol sample) of 4-(methoxycarbonyl)phenyl chloroformate (Fluka) in 50 mL of CH_2Cl_2 was dropped into a solution of 5 g (0.0227 mol) of benzylpiperazinecarboxylate (obtained from piperazine and

benzyl chloroformate at pH 6 as described earlier^{4,9}) in 50 mL of CH_2Cl_2 , followed by the addition of 50 mL of aqueous 1 M Na_2CO_3 . The organic phase was isolated after 1 h of stirring, washed, and dried and the solvent removed in vacuo; yield

82%. $^1\text{H-NMR}$ (CDCl_3): δ = 3.58 (m; $\text{N-CH}_2\text{CH}_2\text{-N-CH}_2\text{CH}_2$, 8 H), 3.90 (s; COOCH_3 , 3H), 5.17 (s; PhCH_2 , 2H), 7.18, 8.06 (dd; PhCOOMe , 4H), 7.37 (m; PhCH_2 , 5H).

Methyl 4-(((Piperazin-1-ylcarbonyl)oxy)benzoate (16) was obtained from 15 by hydrogenation in the presence of Pd/C similarly as described earlier for the deblocking of the secondary amino group;^{4,9} yield 87%. $^1\text{H-NMR}$ (CDCl_3): δ = 2.91 (m; $\text{HN}(\text{CH}_2)_2$, 4H), 3.55–3.64 (m; $\text{N}(\text{CH}_2)_2$, 4H), 3.90 (s; COOCH_3 , 3H), 7.20, 8.04 (dd; Ph , 4H).

Benzyl 4-(Methylcarbamoyl)piperazinecarboxylate (18). A 10 g (45 mmol) sample of 14^{4,9} and 4.6 g of triethylamine in 30 mL of diethyl ether was charged into 20 mL of phosgene/diethyl ether (v/v) at –60 °C. The reaction mixture was thawed, and excess phosgene and ether were removed in vacuo. The residue was extracted three times with dry ether, and gaseous methylamine (Merck) was fed into the ether solution for 10 min. The solution was washed with 100 mL of 1 M H_2SO_4 , dried, and evaporated; yield 34%. $^1\text{H-NMR}$ (CDCl_3): δ = 2.78 (d; NHCH_3 , 3H), 3.36, 3.50 (m; $\text{N-CH}_2\text{CH}_2\text{-N-CH}_2\text{CH}_2$, 8H), 4.8 (s; NH , 1H), 5.14 (s; PhCH_2 , 2H), 7.34 (m; PhCH_2 , 5H).

N-Methyl-piperazinecarboxamide (19). A 4 g (14 mmol) sample of 18 dissolved in 200 mL of acetic acid/methanol (1:1 v/v) and 0.3 g of Pd/C (5%) was charged into a 1 L glass autoclave. The reaction vessel was charged three times with H_2 up to 10 bar followed by a pressure relief and then stirred for 1 h at 56 °C (10 bar initial H_2 pressure). After pressure relief, charging with H_2 (10 bar initial pressure), and another 1 h stirring, the catalyst was removed, the solvent evaporated, and the reaction product (acetate salt) recrystallized from ethanol; yield 72%. $^1\text{H-NMR}$ (CDCl_3): δ = 2.03 (s; CH_3COO^- , 3H), 2.78 (s; NHCH_3 , 3H), 3.13 (s; $\text{H}_2\text{N}^+(\text{CH}_2)_2$, 4H), 3.67 (s; $\text{N}(\text{CH}_2)_2$, 4H), 5.41 (s; NH , 1H).

Hydrobis(1,4-piperazinediylcarbonyloxy-tetramethyleneoxycarbonyl)-N-methyl-piperazine-4-carboxamide (22a)/Hydrobis(1,4-piperazinediylcarbonyloxy-tetramethylene-oxycarbonyl)-[(4-(methoxycarbonyl)-phenyl)oxy]piperazine (22b) were obtained from 16 and 19, respectively, and 20,^{4,9} followed by the removal of the Cbo protecting group from 21a/b by hydrogenation in the presence of Pd/C similarly as described earlier for the stepwise synthesis of oligourethane;^{4,9} yield 70%. $^1\text{H-NMR}$ (CDCl_3): 22a: δ = 1.73 (m; $\text{CH}_2\text{CH}_2\text{CH}_2\text{O}$, 8H), 2.80 (d; NHCH_3 , 3H), 2.90 (t; $\text{HN-}(\text{CH}_2)_2$, 4H), 3.34 (m; $(\text{CH}_2)_2\text{NCONHCH}_3$, 4H), 3.46 (m; $\text{N-CH}_2\text{-CH}_2\text{-N-CH}_2\text{CH}_2$, 16H), 4.14 (m; COOCH_2 , 8H); 22b: δ = 1.73 (m; $\text{CH}_2\text{CH}_2\text{CH}_2\text{O}$, 8H), 2.82 (t; $\text{HN}(\text{CH}_2)_2$, 4H), 3.41–3.7 (m; $\text{N-CH}_2\text{-CH}_2\text{-N-CH}_2\text{CH}_2$, 20H), 4.14 (m; COOCH_2 , 8H), 7.20, 8.04 (dd; PhCOOMe , 5H).

The syntheses of the macromonomers 24a/b, starting from 22a/b and 5 via 23a/b, and of the graft copolymers 1d,e were carried out as described earlier (cf. ref 1).

Acknowledgment. Financial support of this study by the Ministry of Research and Technology (Grant No. 03M40436) and Bayer AG (Leverkusen) is gratefully acknowledged. T.H. wishes to thank the Fonds der Chemischen Industrie for a doctoral fellowship.

References and Notes

- Eisenbach, C. D.; Heinemann, T. *Macromolecules* **1995**, *28*, 2133.
- Eisenbach, C. D.; Heinemann, T.; Ribbe, A.; Stadler, E. *Macromol. Symp.* **1994**, *77*, 125.
- Harrell, L. L., Jr. *Macromolecules* **1969**, *2*, 607.
- Eisenbach, C. D.; Nefzger, H. In *Contemporary Topics in Polymer Science*; Culbertson, W. M., Ed.; Plenum Publishing Corp.: New York, 1989; Vol. 6, p 339.
- Kornfield, J. A.; Spiess, H. W.; Nefzger, H.; Hayen, H.; Eisenbach, C. D. *Macromolecules* **1991**, *24*, 4185.

- (6) Eisenbach, C. D.; Nefzger, H.; Hayen, H.; Enkelmann, V. *Macromol. Chem., Phys.* **1994**, 195, 3325.
- (7) Saari, W.; Raab, A.; King, S. *J. Org. Chem.* **1971**, 36, 1711.
- (8) Jucker, E.; Rissi, E. *Helv. Chim. Acta* **1962**, 45, 2383.
- (9) Eisenbach, C. D.; Stadler, E.; Enkelmann, V. *Macromol. Chem., Phys.* **1995**, 196, 833.
- (10) Tilley, J. N.; Sayigh, A. *J. Org. Chem.* **1963**, 28, 2076.
- (11) Eisenbach, C. D.; Baumgartner, M.; Günther, G. In *Advances in Elastomers and Rubber Elasticity*; Lal, J., Mark, J. E., Eds.; Plenum Publishing Corp.: New York, 1987; p. 51.
- (12) Seefried, C. G.; Koleske, J. V.; Critchfield, F. E. *J. Appl. Polym. Sci.* **1975**, 19, 2493.
- (13) Senich, G. A.; MacKnight, W. J. In *Advances in Chemistry*; Cooper, S. L., Estes, G. M., Eds.; American Chemical Society: Washington, DC, 1979; Vol. 176, p 97.
- (14) Ng, H. N.; Allegrezza, A. E.; Seymour, R. V.; Cooper, S. L. *Polymer* **1973**, 14, 225.
- (15) Eisenbach, C. D.; Gronski, W. *Makromol. Chem. Rapid Commun.* **1983**, 4, 707.
- (16) Eisenbach, C. D.; Heinemann, T.; Ribbe, A.; Stadler, E. *Angew. Makromol. Chem.* **1992**, 202/203, 221.
- (17) Eisenbach, C. D.; Heinemann, T. *Macromol. Chem., Phys.* **1995**, 196, in press.
- (18) Wurziger, H. *Kontakte (Darmstadt)* **1987**, 3, 8.
- (19) Karrer, P.; Nicolaus, B. *Helv. Chim. Acta* **1952**, 35, 1581.
- (20) Magnier, E.; Baltzly, R. *J. Org. Chem.* **1958**, 23, 2029.

MA946515Q